UNIVERSITY OF CALIFORNIA
SANTA CRUZ

QUANTIFYING ATMOSPHERIC MICROPLASTIC CONCENTRATIONS AT TWO SITES IN CALIFORNIA

A thesis submitted in partial satisfaction
of the requirements for the degree of

MASTER OF SCIENCE

in

EARTH SCIENCES

by

Lauren Hashman

June 2024

The Thesis of Lauren Hashman
is approved by:

Dr. Adina Paytan, chair

Dr. Peter Weiss

Dr. Jeremy Hourigan

Peter Biehl
Vice Provost and Dean of Graduate
Studies

Table of Contents

List of Figures

Abstract

Quantifying Atmospheric Microplastic Concentrations at Two Site in California

Lauren Hashman

Micro- (<5mm diameter) and nano-plastics (1nm-1 μm diameter) are ubiquitous pollutants to aquatic and terrestrial environments and these particles can be transported long distances through the atmosphere. While not fully understood, microplastics are potentially detrimental to the health of humans and animals. This study compares atmospheric microplastic particles (AMP) concentrations collected from air samples over terrestrial and coastal regions in California: Lake Tahoe and Monterey Bay, respectively. Atmospheric total suspended particulate matter was collected weekly at the three site locations and AMP concentration in samples from 2006 to 2023 were determined using flow cytometry to quantify concentrations and track changes in plastic particle abundance over time. NOAA HYSPLIT back trajectories are used to infer probable AMP source regions. The coastal sites of Santa Cruz and Elkhorn Slough Reserve are proximal to different land usage with similar distances to the coast. Lake Tahoe is 285 km from the ocean and an altitude of 1897 m. Lake Tahoe samples recorded an average concentration of 2.39 particles m^{-3} from 2005-2006 and 1.83 particles m^{-3} from January-October 2009. Elkhorn Slough Reserve recorded an average concentration of 4.56 particles m^{-3}. Samples collected before and after a large wildfire at the Santa Cruz Mountains were also compared. Santa Cruz recorded an average of 8.44 particles m^{-3} prior to the CZU fire complex, 17.59 particles m^{-3} during and 4.93 particles m^{-3} directly after. Higher AMP

concentrations at all three sites correspond to long range transport with local and regional (urban, wildfire) influence. This study aims to detect AMP in locations with varying proximity to the ocean and land use in hopes to draw awareness about how long-range transport of AMP is affecting the environment and subsequently the public's health.

Dedication and Acknowledgments

I would like to thank my advisor Adina Paytan for the constant support and guidance throughout my academic pursuit.

I would like to thank Eyal Rahav and his team at the Israel Oceanographic & Limnological Research Institute for their contribution the research.

The authors gratefully acknowledge the NOAA Air Resources Laboratory (ARL) for the provision of the HYSPLIT transport and dispersion model and/or READY website (https://www.ready.noaa.gov) used in this publication.

Introduction

The global plastic production is predicted to reach 940 million Mt in 2024 (Surendran et al., 2023). Of the plastic produced, 90 Mt could contribute to plastic pollution by 2030 (Borelle et al. 2020). Macro-plastics can undergo physical or chemical degradation resulting in smaller plastic pollution fragments (micro- and nano-) which are abundant in every environmental medium. Microplastics include plastic particles with a diameter ranging between 1 μm and 5 mm. 'Primary' microplastics are classified by plastic particles manufactured to the size range of 1μm-5 mm (Allen et al., 2022). Primary microplastics enter the environment directly as particles in the calcified size range and usually originate from domestic products (beauty products, textiles) and introduced to the environment via our wastewater system (Horton & Dixon, 2017). 'Secondary' microplastics are derived from either physical or chemical degradation of larger plastic pieces to the micro-size range (Allen et al. 2020). Secondary microplastics are typically introduced to the environment by pollution (either intentional or mismanaged) (Boucher & Friot, 2017). Microplastics have been detected and studies in soil (Sajjad et al., 2022), fresh aquatic environments (Li et al., 2018) and marine systems (Cole et al., 2011), biota (Hermsen et al., 2018) including in humans (Zhu et al., 2024) and within the atmosphere (O'Brien et al., 2023). The atmosphere is an important medium of microplastic dispersal hence focus on atmospheric microplastic is growing rapidly, with the 70 peer reviewed articles of field and laboratory research published in 2020 increasing to 124 published sources by 2022 (Allen et al., 2020, O'Brien et al., 2023).

The amount of visible plastic pollution in the surface environment does not always correlate with the amount of plastic pollution in the atmosphere due to the diverse sources and transport mechanisms of microplastic (Brahney et al., 2020).

The size and density of microplastic particles allows for plastic pollution to enter the atmosphere from surface sources. The surface ocean is an important source of microplastic particles to the atmosphere and AMP are transported with the wind to terrestrial environments as well. Allen et al., (2020) utilize the established model of sea salt aerosols formation to model the ocean-atmosphere microplastic transfer flux. Marine plastic pollution (micro- to nano-) enters the atmosphere by bubble bursting and jet expulsion (Allen et al., 2020). Particles up to 20 μm can be ejected by wave action and dispersed by the wind like other aerosol particles. Microplastic particles float in seawater; wind action can uplift these particles providing another pathway for the introduction of microplastics from the marine environment to the atmosphere. The ocean-atmosphere transfer can be exacerbated in coastal environments due to higher wave action (Allen et al., 2022). Indeed, a study done in the Baltic Sea (Ferrero et al., 2022), atmospheric microplastic accumulation was higher at the coastal site of Gdansk harbor (161 ± 75 m^{-3}) than in the open Baltic Sea (24 ± 9 m^{-3}). On the surface of Germany's Rhine River, an average of 892,777 microplastic particles km^{-2} were found (Mani et al., 2015). Microplastics can be detected in influent (untreated in flow) and effluent (treated discharged) water in wastewater treatment plants (Sun et al., 2019). Wind over land can also introduce microplastics into the air. A study done on agricultural land exposed to erosive winds recorded 0.08-1.48 mg m^{-3} min^{-1}

microplastics emission (Rezaei, 2019). Microplastics are introduced to the agricultural soil environments from polyethylene plastic mulching (He et al., 2018). Cities and urban development areas have varying atmospheric microplastic accumulation, with a study in Paris reporting 0.9 particles m^{-3} (Dris et al., 2017) and in a study Beijing reporting 5,700 particles m^{-3} (Li et.al, 2020). Remote terrestrial and marine environments are subject to atmospheric microplastic pollution despite 'pristine' air quality conditions, which typically consider only gas and smog pollution, due to long range atmospheric transport. A study done by Allen et.al in 2020 detected 0.09-0.66 microplastic particles m^{-3} air in the remote French Pyrenees and attributed this to long-range transport. In remote areas in the western United States an average of 132 particles m^{-2} day^{-1} were detected (Brahney et al., 2020), suggesting long-range transport of atmospheric microplastics to remote terrestrial environments. A model to constrain point source emission of atmospheric microplastics in the western United States concluded that 84% of atmospheric microplastics originate from road dust sources, 11% from the ocean and 5% from agricultural development (Brahney et al., 2021). California AMP pollution has been detected on a small scale; California State University, California detected 9.8 ± 7.8 particles m^{-3} (fibrous) and 6.8 ± 5.2 particles m^{-3} (fragments) (Gaston et al., 2020). In this paper we compare the abundance of microplastics at three sites characterized by different land-use, land-cover and distance from the ocean in California to assess the effect of these variables on microplastic in the air. We also report data from samples collected during a wildfire (CZU Lightning Complex fires of 2020) for comparison.

Methods:

Total suspended particles were collected at three sites in California, Lake Tahoe, Elkhorn Slough Reserve near Moss Landing and on the Coastal Science Campus of UCSC in Santa Cruz (Figure 1). The sites represent differing settings that could contribute to atmospheric microplastic emissions and deposition. Lake Tahoe, Elkhorn Slough and Santa Cruz are located at varying distances from the Pacific Ocean; the Santa Cruz sampling site is located on a cliff close to the water line (~17 m), the Elkhorn Slough site is within the Elkhorn Slough Reserve about 5 km inland from the Moss Landing Harbor.

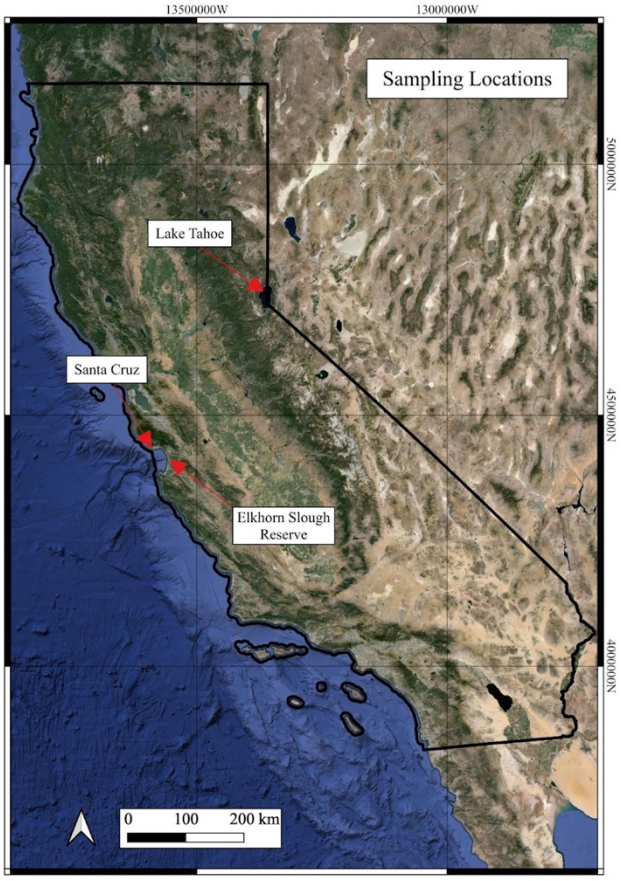

Figure 1: Map of sampling location in California. Lake Tahoe is situated in the Sierra Nevada Mountains near the California-Nevada border. Santa Cruz and Elkhorn Slough Reserve are coastal sites on the Monterey Bay.

Lake Tahoe is situated approximately 285 km from the California coast. Lake Tahoe (pop. ~ 21,000) is in the Sierra Nevada mountains with nationally protected forests (Figure 2) to the west and the sparsely populated Great Basin Desert to the

east. Tahoe hosts approximately 15 million tourists annually; with plenty of lodging options, popular summer and winter recreation, Lake Tahoe can reach 300,000 tourists in a day (The Tahoe Fund website 2024).

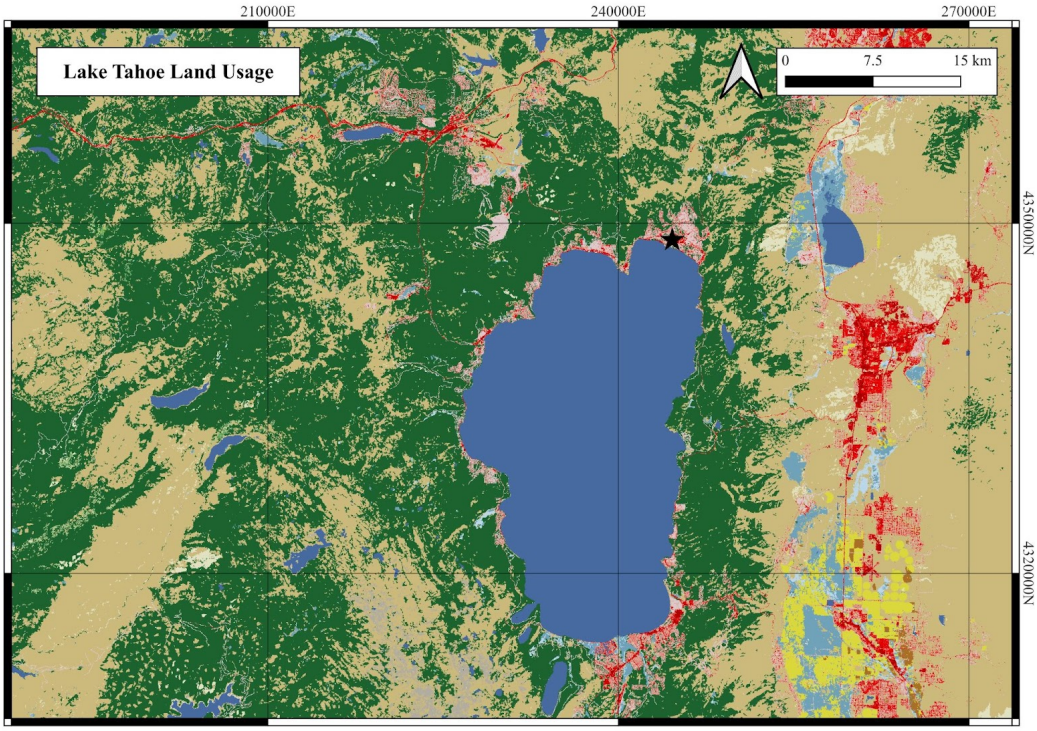

Figure 2: Map of land use practices of the greater Lake Tahoe Basin area using NLCD (Dewitz & U.S. Geological Survey, 2021). Sampler location indicated by the black star. The corresponding color classifications, as provided by the NLCD (Dewitz & U.S. Geological Survey, 2021), are presented in Figure 5.

Elkhorn Slough Reserve is a nationally protected sanctuary; however, it is proximal to agriculture land (strawberries, artichokes, leafy greens). Elkhorn Slough is also proximal to urban development with the nearest city being Watsonville, California approximately 10 km to the north (Figure 3) but is frequented by visitors and kayakers.

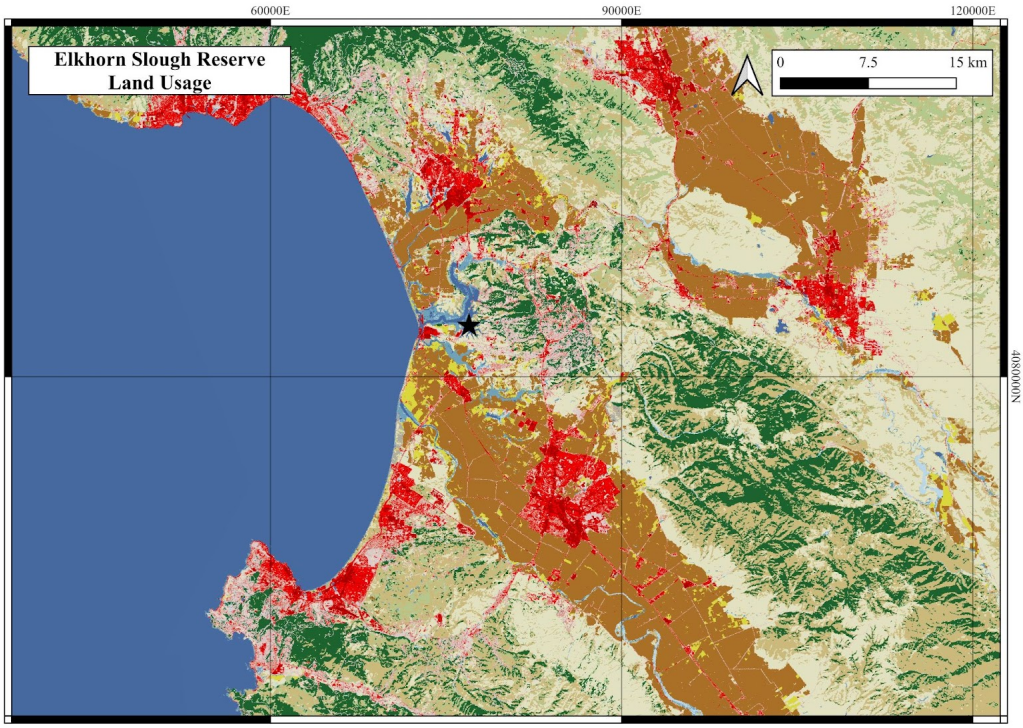

Figure 3: Map of land use practices of the Elkhorn Slough Reserve and surrounding areas. The black star indicates sampler location. Northwest of the sampler location (beneath the map title) lies the city of Santa Cruz, while the city of Monterey is to the southwest. The corresponding color classifications, as provided by the NLCD (Dewitz & U.S. Geological Survey, 2021), are presented in Figure 5.

Santa Cruz (pop. ~61,950) is at the northern headland of Monterey Bay, the surrounding land use is dominated by forested mountains to the northeast and the prevailing wind direction is from the ocean (Figure 4).The National Land Cover Dataset (NLCD) (Figure 5) (Dewitz & U.S. Geological Survey, 2021) of the sampling

locations paired with back trajectory analysis is presented in Figure 6, to demonstrate the potential influence of land use on atmospheric microplastic concentrations.

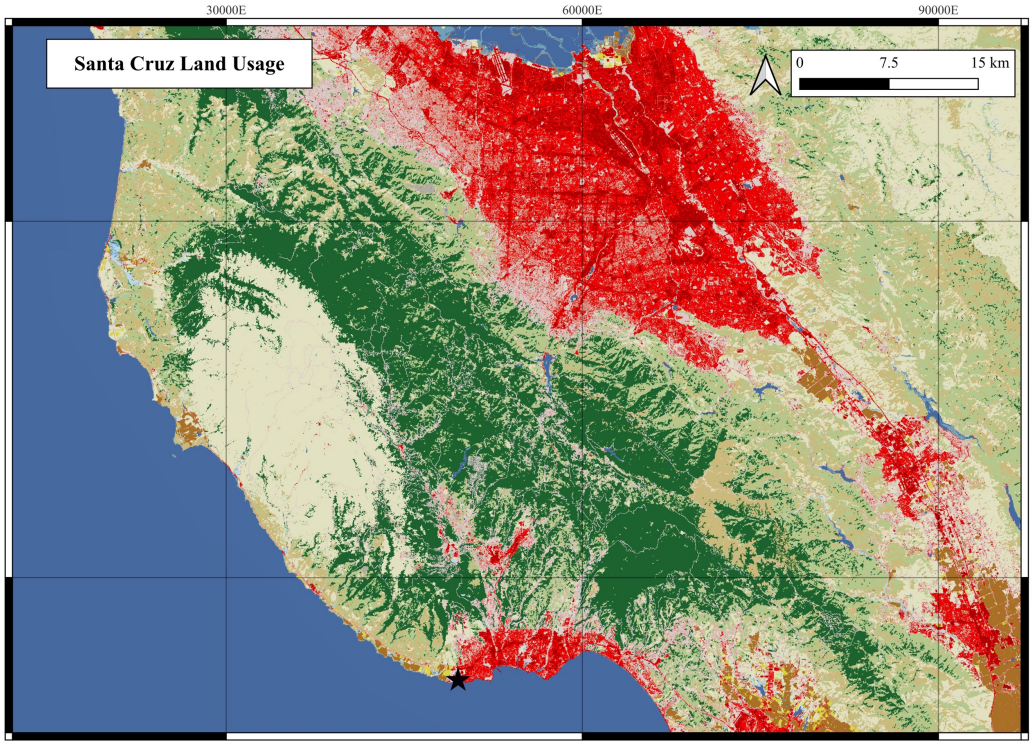

Figure 4: Map of land use practices of Santa Cruz with the black star indicating sampler location. Map includes the Greater San Jose Metropolitan Area to the north. The corresponding color classifications, as provided by the NLCD (Dewitz & U.S. Geological Survey, 2021), are presented in Figure 5.

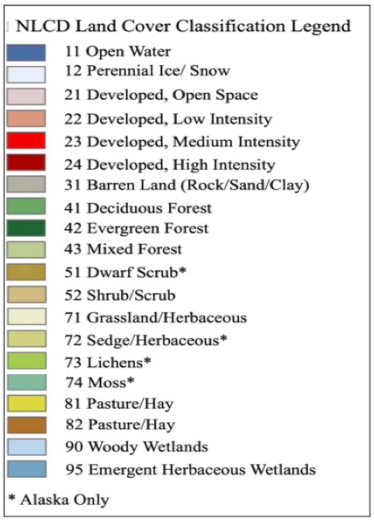

Figure 5: Color classification legend of the 2021 National Land Cover Dataset (NLCD), retrieved from Jon Dewitz and the U.S. Geological Survey [10]

Back trajectory analysis for each sampling period was used to determine possible land range emission sources of atmospheric microplastics. The NOAA HYSPLIT back trajectory model was set with with a 48-hour run time to determine the origin of air masses before collection (Stein et al., 2015; Rolph et al., 2017). The GDAS1 database provided by NOAA was used to obtain back trajectory information for all three locations. The GDAS database runs 4 times a day with an output of 6-hour forecasts. The frequency grid resolution for the model is 1.0 degrees; the frequency plot uses model vertical velocity motion and a height of 500 m above ground level. This method does not depict the surface-atmosphere microplastic flux accurately; rather this was used as a preliminary model to attempt to connect high AMP concentrations to areas of urban development. In a study done by Steve Allen (2020), modal trajectory elevation of AMP interacts with the surface at 60-72 hours before reaching the sampler in the remote Pyrenees Mountains (altitude ~3404 m); at this time, it is also suggested that there is mixing of microplastics into the planetary boundary level (Allen, 2020). The back trajectory plots associated with the samples were observed visually to estimate influences on AMP pollution (Figure 6). Samples were categorized into surface land uses practices associated with 70-90% range on the frequency plots; while it is unlikely that surface land use practices are directly influencing AMP concentration, this method was used as an estimate. The model in this study runs for 48 hours before sample was collected; the frequency plot chosen was the number of endpoints per grid square divided by the maximum number of endpoints in any grid square to receive the maximum frequency a trajectory passes

over a grid cell. It should be noted that AMP can travel 10-1000 km (Allen et al., 2020). Residence time of atmospheric microplastics has not been well defined until recently, but the observance at remote locations suggests long range transport. A new study by E. Ward et al. (2024) looking at spherical polystyrene atmospheric microplastics report particulate matter ($PM_{2.5}$ and PM_{10}) microplastics have a residence time in the atmosphere of 28 to 8 days. The back trajectory information we used was the last 48 hours before collection date which does not guarantee a location signal but rather focuses on local microplastic movement in the atmosphere.

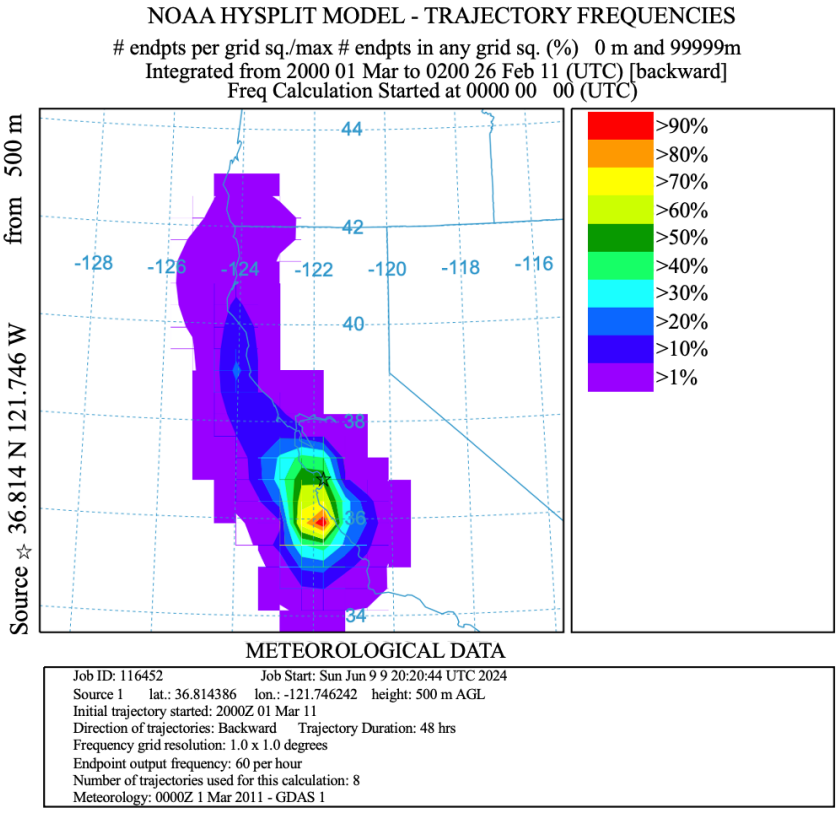

Figure 6: Example back trajectory frequency plot from the NOAA HYSPLIT GDAS1 database [23][28]. The endpoint location, marked by the star, is the Elkhorn Slough Reserve. The trajectory ends on the sample collection date, March 1st, 2011. The color classification on the left depicts the frequency an air parcel passes over each grid cell. This particular trajectory is categorized under the 'marine with urban influence' (Figure 14) land use as over 60% of the air parcel's path travels over Monterey, California.

Aerosols particulate matter samples are collected using high-volume total suspended particle aerosol samplers (Figure 7). Flow rates differ between sampling locations: Lake Tahoe 84.96 m^3 hr^{-1}, Elkhorn Slough Reserve 84 m^3 hr^{-1}, Santa Cruz 84.96 m^3 hr^{-1}(2019-2020). Environmental samples are collected on QM-A quartz filters. The auxiliary data from the sampling duration is recorded before samples are stored in either Low-Density Polyethylene bags (Tahoe) or aluminum foil (Elkhorn Slough Reserve and Santa Cruz). Two control filters were placed in Low-Density Polyethylene bags for 1 and 3 years were used to account for possible microplastic influence from the storage mechanism of the Tahoe samples. Samples are from archive datasets; the gap in time in the Lake Tahoe dataset (2005-2006 to 2009) is because these archive samples had the most continuous time series. The goal was to have overlapping time between the Lake Tahoe and Elkhorn Slough datasets; the auxiliary data of the Lake Tahoe samples (November 2009 to February 2010) did not have total volume values, making it impossible to calculate the particle accumulation per cubic meter of air.

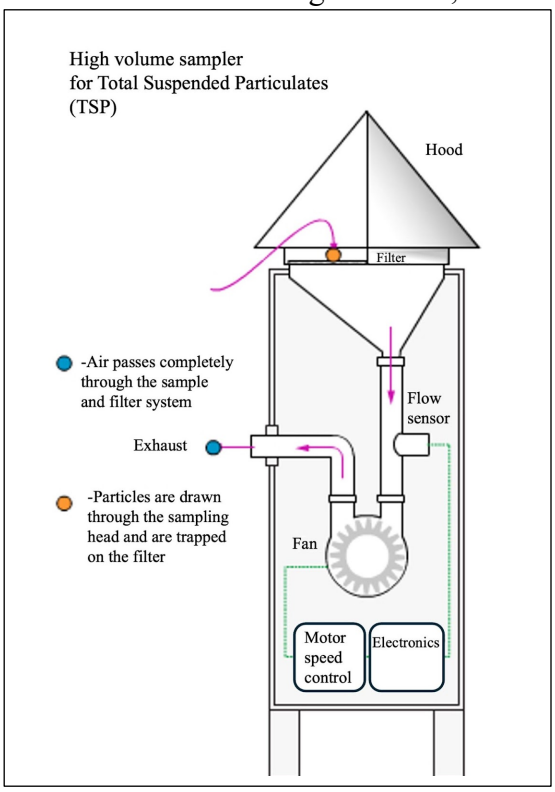

Figure 7: Illustration of the basic mechanism for a high-volume sampler for total suspended particulates [29].

Sections of 7.5 cm^2 were cut from the environmental filter sample and added to glass vials filled with deionized water. The vials are placed in an ultrasonic bath for one hour to remove the particles from the filter matrix (Bein & Wexler, 2014). Before adopting this method, filter segments from the Lake Tahoe 2005-2006 time series were examined using optical microscopy both before and after sonication to confirm resuspension of particulate matter. After sonication, the solution for sections from the same filter were combined and the solutions were refiltered onto 47 mm GF-F filters for further analysis. Samples were sent to the Israel Oceanographic & Limnological Research Institute for further dyeing and microplastic concentration analysis. Samples are dyed with a 10 mg/mL Nile Red dye solution with 1:1 Acetone:Ethanol (Liu et al., 2021) for Flow-Cytometry Analysis. Total volume of air that flows through the sample is found by the run time of the sampler multiplied by the sampler flow rate. The product of the relative digested filter area (7.5 cm^{-2} / total filter area) multiplied by the total volume gives us the actual volume of air that passes through digested filter segments. Blank filter controls and instrument blanks corresponded to a maximum of 9.56 particles m^{-3}. The value of 9.5 particles m^{-3} subtracted from the absolute particle read from the Flow-Cytometry Analysis then divided by the actual volume to yield a value of particles m^{-3}.

Results:

The average microplastic concentration of Lake Tahoe in 2005-2006 was 2.39 particles m^{-3} with a maximum concentration of 6.72 particles m^{-3} (Figure 8). The back

trajectory showed that >90% of the air parcel associated with the maximum concentration originated from Sacramento, California. Samples collected in Autumn (October-December) had the highest AMP concentrations for this sampling period. Figure 9 segregates sample AMP concentrations by surface land use practices.

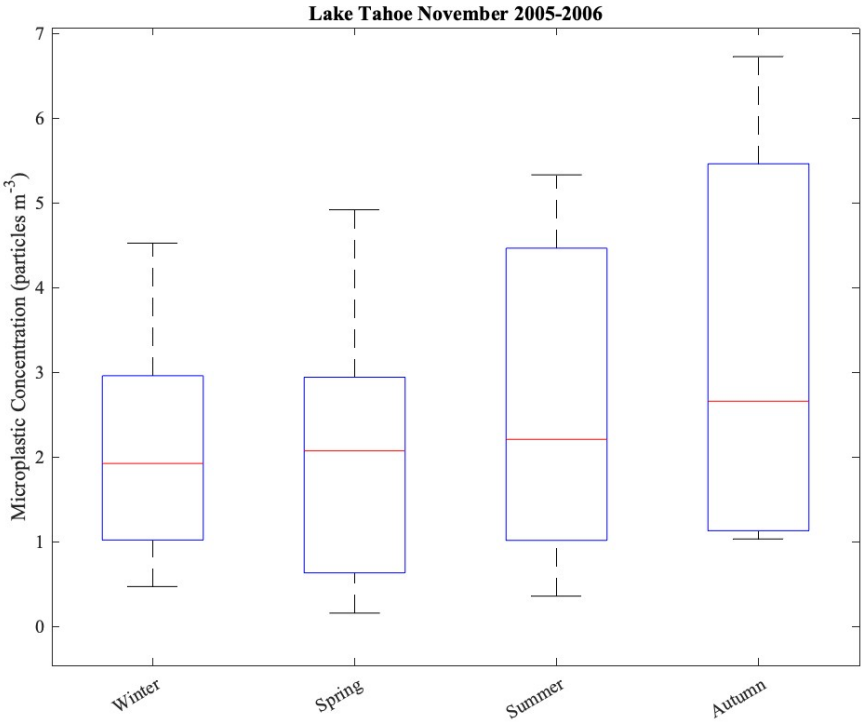

Figure 8: Lake Tahoe (2005-2006) AMP concentrations (particles m^{-3}) segregated by seasons.

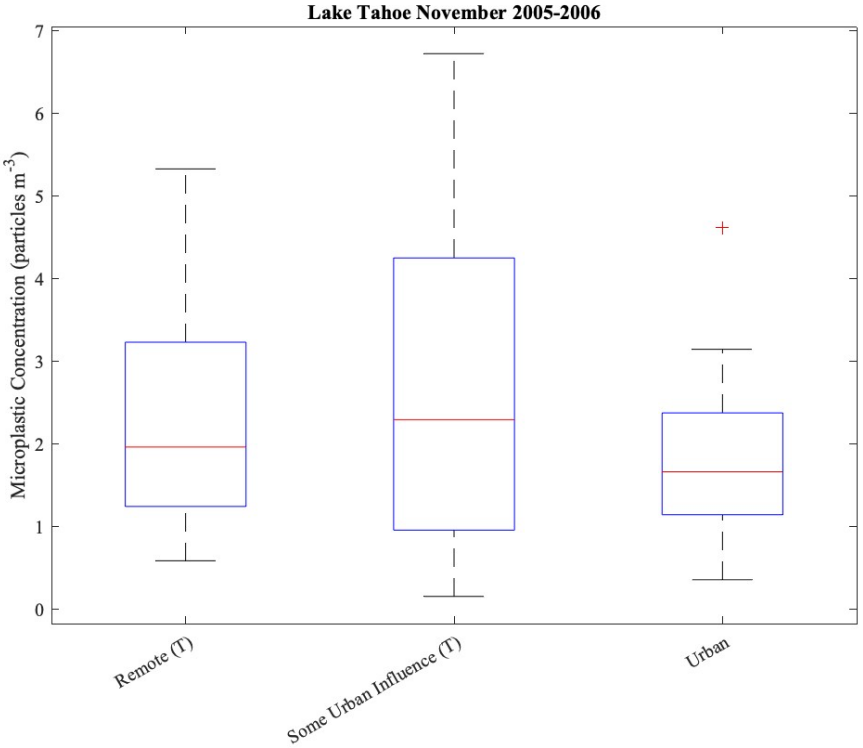

Figure 9: Lake Tahoe (2005-2006) AMP concentrations (particles m^{-3}) segregated by surface land use practices.

The average microplastic concentration for Lake Tahoe in 2009 is 1.83 particles m^{-3}. and maximum microplastic concentration in 2009 is 8.59 particles m^{-3} (Figure 10). The back trajectory associated with the maximum concentration showed that >90% of the air parcel originated from the Central Valley of California, where population is relatively low but agricultural development is high. Majority of the Tahoe samples from both sampling periods 2005-2006 and 2009 are of terrestrial origin including agriculture and urban influence (Figure 9 & 11).

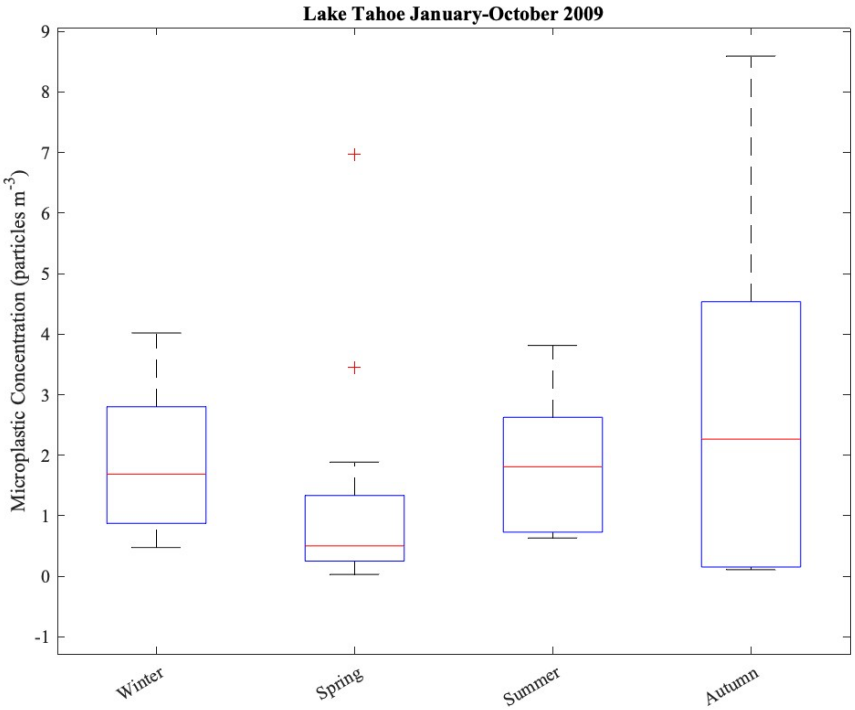

Figure 10: Lake Tahoe (January-October 2009) AMP concentrations segregated by season.

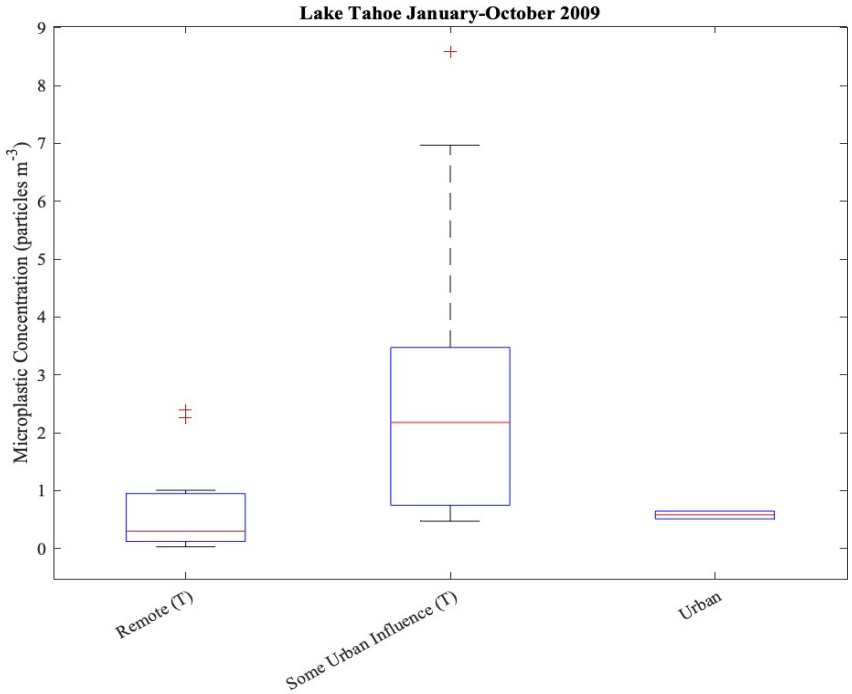

Figure 11: Lake Tahoe (January-October 2009) AMP concentrations segregated by surface land use practices.

Rose diagrams of the air parcel back trajectory directions for the sampling years are presented in Figure 12. Back trajectory direction for each sample was estimated using the frequency plots. Air parcel back trajectory is predominantly to the south and within the Tahoe Basin. Air mass back trajectory originating from the southwest corresponds to the greater Sacramento and Central Valley areas.

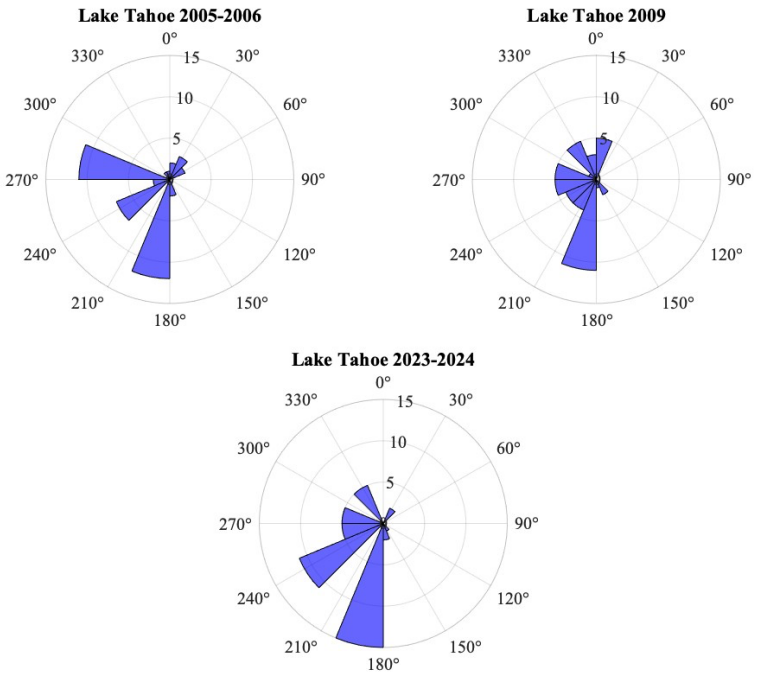

Figure 12: Rose Diagram (polar histogram) of back trajectory directions for the two sampling periods (top) and for the previous year (bottom) for Lake Tahoe.

The average microplastic concentration of Elkhorn Slough Reserve from 2010-2011 is 4.6 particles m^{-3} with a maximum concentration of 31.22 particles m^{-3}. As seen in Figure 13, the AMP concentrations are relatively consistent throughout the seasons. The back trajectory associated with the maximum concentration showed primarily marine origin with >50% of the air parcels having minor urban influence as well. Air parcel back trajectories of urban origin seem to be associated with higher

microplastic concentrations (Figure 14) but cannot be confirmed without further statistical testing. Of the samples with urban origin, the median value is 5.95 particles m^{-3} and the maximum is 22.38 particles m^{-3}. Figure 15 compares the air parcel trajectories of the sampling duration to that of 2023-2024. The dominating air parcel trajectory in both time intervals originates from the northwest, which is the back trajectory direction associated with the maximum microplastic concentrations with marine and urban influence 2010-2011 (Figure 14).

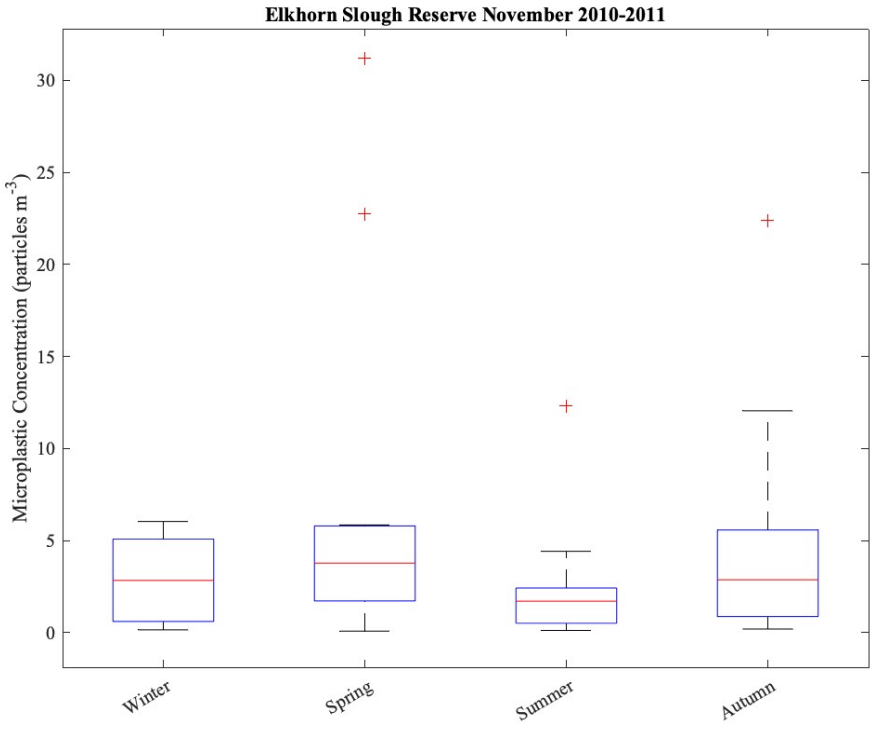

Figure 13: Elkhorn Slough Reserve (2010-2011) AMP concentrations segregated by season.

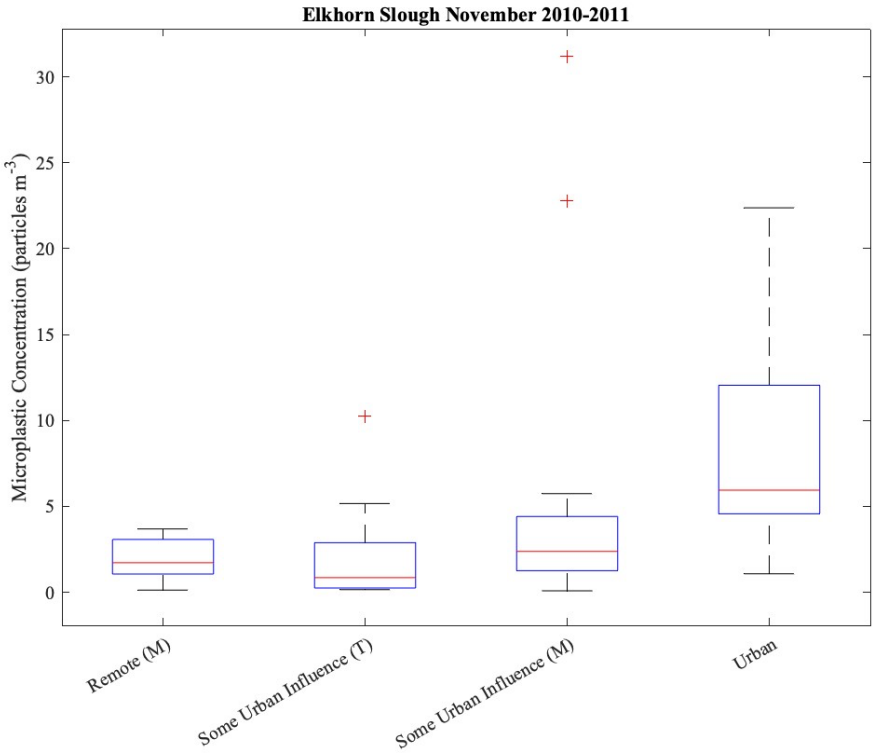

Figure 14: Elkhorn Slough Reserve (2010-2011) AMP concentrations segregated by surface land use practices.

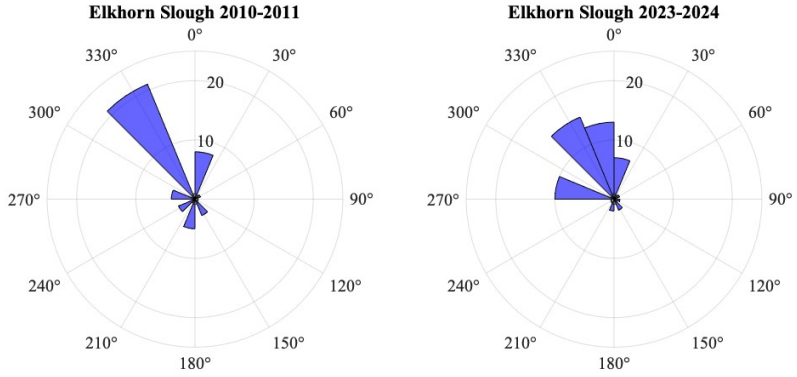

Figure 15: Rose Diagrams (polar histograms) of the back trajectory directions for the sampling duration and the previous year at the Elkhorn Slough Reserve.

The average AMP concentration in Santa Cruz from October 2019-2020 was 8.68 particles m^{-3} with the highest concentrations being during the summer (Figure 16). Figure 17 compares the AMP concentrations relative to the 2020 CZU Lightning Complex fires. The microplastic concentration in Santa Cruz before the fires (October 8th, 2019, to August 15th, 2020) was 8.44 particles m^{-3} on average. The highest microplastic concentration of 44.21 particles m^{-3} showed >90% of air parcel back trajectory originating from Santa Cruz city with some urban influence from Silicon Valley. The CZU Lightning Complex fires burned 86,509 acres in Santa Cruz and San Mateo County for 37 days (Cal Fire). The average microplastic concentration rose to 17.59 particles m^{-3} during the fires (August 29th to September 20th, 2020). Directly after the fires the microplastic concentration dropped to 4.93 particles m^{-3}. Samples following the fire that were of terrestrial origin had higher AMP concentrations (i.e. 7.37 and 9.87 particles m^{-3}); samples of marine origin showed lower concentrations like 0.93 and 1.94 particles m^{-3}. Many samples are of terrestrial origin with some urban influence despite the proximity of the site to the ocean (Figure 18). The majority air parcel direction between 2019-2020 and 2023-2024 is north (Figure 19), signifying the influence of urban pollution at this location.

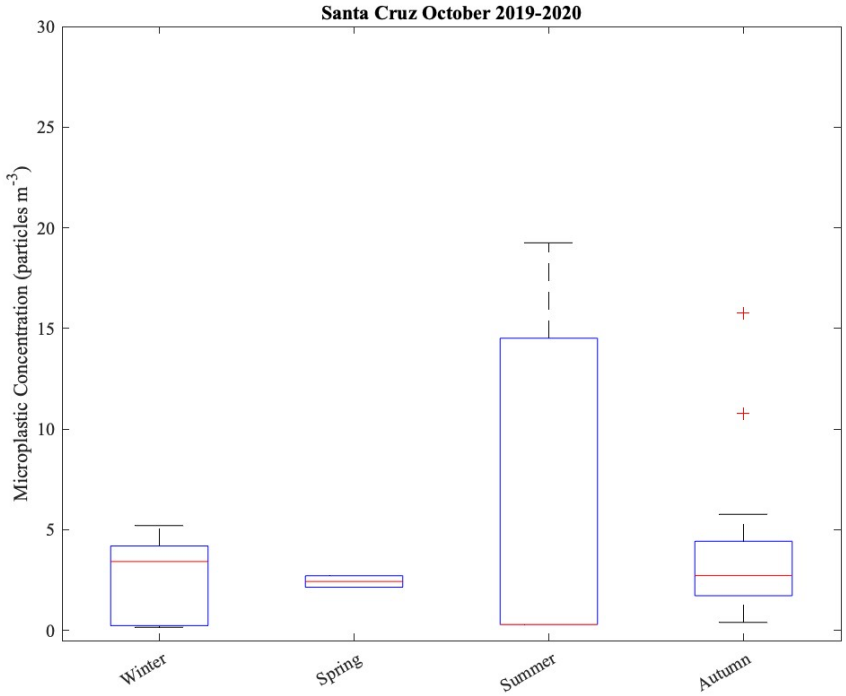

Figure 16: Santa Cruz (2019-2020) AMP concentrations segregated by season.

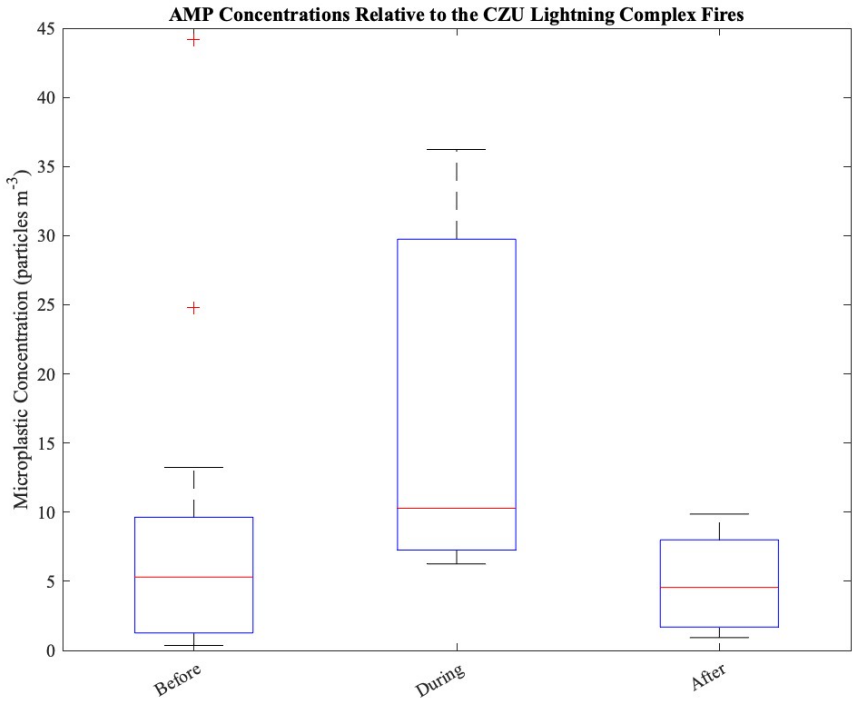

Figure 17: Santa Cruz (2019-2020) AMP concentrations relative to the CZU Lightning Complex Fires

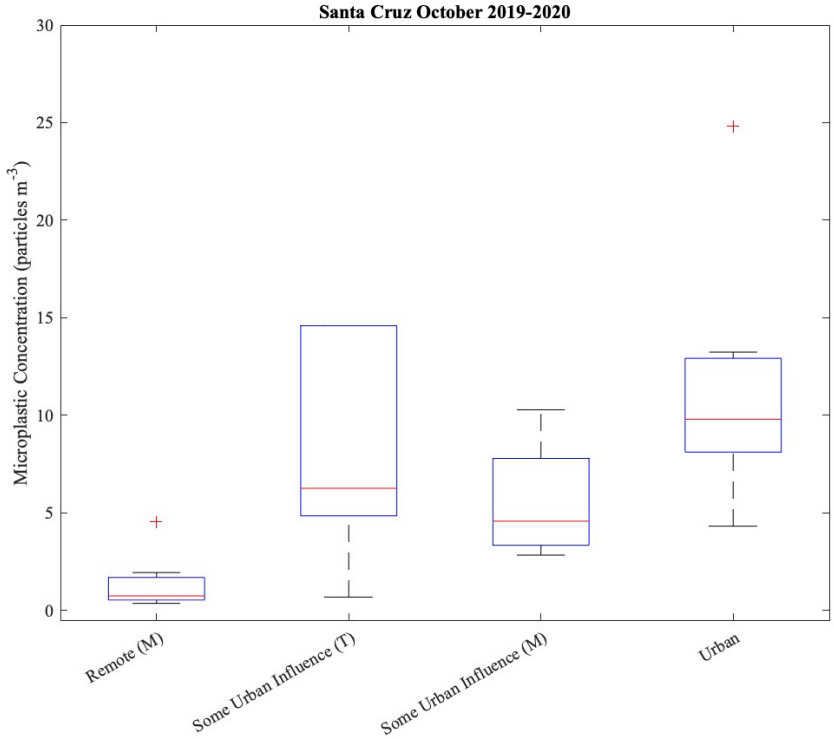

Figure 18: Santa Cruz (2019-2020) AMP Concentrations segregated by surface land use practices.

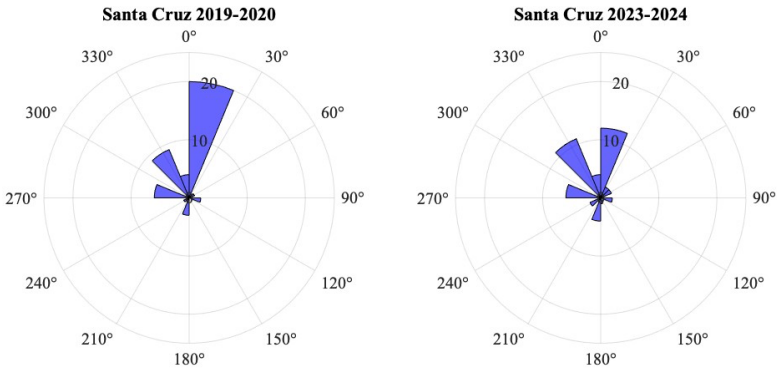

Figure 19: Rose Diagrams (polar histograms) of the back trajectory directions for the sampling duration and the previous year.

Discussion:

The sample locations in this study are all considered ‘pristine’ by global standards. The atmospheric microplastic concentrations are relatively low compared to other studies; the back trajectory analysis shows that long range transport of microplastics could be contributing to atmospheric microplastic concentrations, accumulating in pristine environments and impacting the people and ecosystems in these areas.

High AMP concentrations in these areas are not a result of proximal plastic pollution but rather the long-range transport of these materials. The CZU Lightning Fire Complex directly influenced the amount of microplastics in the air due to the incineration of ground material and increase of suspended particulate matter (Figure 17). Despite the obvious AMP increase due to the fires, the highest AMP concentrations in Santa Cruz originate from land use practices beneath air parcel trajectory. AMP concentrations rise significantly if the back trajectory originates from land or urban areas compared to marine origin.

As seen in the Elkhorn Slough Reserve samples, minor urban influences (i.e. agricultural development and small cities) seem to influence AMP concentrations. The highest AMP concentrations in Elkhorn Slough have mixed marine and urban influence; AMP concentration of 31.22 particles m^{-3} showed influence from Monterey Bay but also the city of Monterey, California. The AMP concentration of 22.77 particles m^{-3} had influence from the neighboring city of Watsonville, an area of high agricultural development and Santa Cruz.

The Lake Tahoe AMP concentrations seemingly decrease with time; without a continuous time, series it is difficult to draw any conducive conclusions regarding the microplastic concentration throughout time. The rose diagrams of the locations are to draw correlations between land use practices influencing AMP concentrations during the sampling duration and present day in lieu of present-day AMP concentrations. The dominating air parcel back trajectory direction remains seemingly constant throughout time with some natural variability. Without further analysis regarding other meteorological trends of the sites, the back trajectory directions that pose the greatest AMP concentrations cannot be determined.

Conclusion:

With the increasing amount of plastic pollution in the environment, AMP pollution will plague areas we deem as 'pristine'. Our data shows significant differences temporally at each site as well as differences between sites. Due to this variability to assess impacts it is imperative to include high frequency monitoring of AMP possibly combined with air monitoring of TSP. In addition, it is important to conduct studies that can identify and predict the drivers for AMP content at each location and regionally to ensure that measures are taken to reduce AMP impacts on human and ecosystem health. While AMP pollution can only be quantified, making sure plastic pollution stays out of the environment is the only way to ensure AMP concentrations remain low.

References

1. Allen, S. (2020). *Atmospheric Microplastic Pollution* [Doctoral Thesis, University of Strathclyde]. STAX. https://doi.org/10.48730/c5tt-bc60

2. Allen S, Allen D, Moss K, LeRoux G, Phoenix VR,Sonke JE(2020) Examination of the ocean as a source for atmospheric microplastics. PLoS ONE15(5): e0232746. https://doi.org/10.1371/journal.pone.0232746

3. Allen, S., Allen, D., Baladima, F. et al. Evidence of free tropospheric and long-range transport of microplastic at Pic du Midi Observatory. Nat Commun 12, 7242 (2021). https://doi.org/10.1038/s41467-021-27454-7

4. Allen, D., Allen, S., Abbasi, S. et al. Microplastics and nanoplastics in the marine-atmosphere environment. Nat Rev Earth Environ 3, 393–405 (2022). https://doi.org/10.1038/s43017-022-00292-x

5. Bein, K. J., & Wexler, A. S. (2014). A high-efficiency, low-bias method for extracting particulate matter from filter and impactor substrates. *Atmospheric Environment*, *90*, 87–95. https://doi.org/10.1016/j.atmosenv.2014.03.042

6. Borrelle, S. B. et al. Predicted growth in plastic waste exceeds efforts to mitigate plastic pollution. Science 369, 1515–1518 (2020).

7. Boucher, J., & Friot, D. (2017). Primary microplastics in the oceans: A global evaluation of sources. Gland, Switzerland: IUCN.

8. Brahney, J., Hallerud, M., Heim, E., Hahnenberger, M., & Sukumaran, S. (2020a). Plastic rain in protected areas of the United States. *Science*, *368*(6496), 1257–1260. https://doi.org/10.1126/science.aaz5819

9. Brahney, J., Mahowald, N., Prank, M., Cornwell, G., Klimont, Z., Matsui, H., & Prather, K. A. (2021). Constraining the atmospheric limb of the plastic cycle. Proceedings of the National Academy of Sciences, 118(16). https://doi.org/10.1073/pnas.2020719118

10. *Czu lightning complex (including Warnella Fire)*. Cal FIRE. https://www.fire.ca.gov/incidents/2020/8/16/czu-lightning-complex-including-warnella-fire

11. Cole, M., Lindeque, P., Halsband, C., & Galloway, T. S. (2011). Microplastics as contaminants in the marine environment: A Review. *Marine Pollution Bulletin*, *62*(12), 2588–2597. https://doi.org/10.1016/j.marpolbul.2011.09.025

12. Dewitz, J., and U.S. Geological Survey, 2021, National Land Cover Database (NLCD) 2019 Products (ver. 2.0, June 2021): U.S. Geological Survey data release, https://doi.org/10.5066/P9KZCM54

13. Dris, R. et al. A first overview of textile fibers, including microplastics, in indoor and outdoor environments. Environ. Pollut. 221, 453–458 (2017)

14. Ferrero, L. et al. Airborne and marine microplastics from an oceanographic survey at the Baltic Sea: an emerging role of air–sea interaction. Sci. Total Environ. 9, 153709 (2022).

15. Gaston, E., Woo, M., Steele, C., Sukumaran, S., & Anderson, S. (2020). Microplastics differ between indoor and outdoor air masses: Insights from multiple microscopy methodologies. *Applied Spectroscopy*, *74*(9), 1079–1098. https://doi.org/10.1177/0003702820920652

16. He, D., Luo, Y., Lu, S., Liu, M., Song, Y., & Lei, L. (2018). Microplastics in soils: Analytical methods, pollution characteristics and ecological risks. TrAC Trends in Analytical Chemistry, 109, 163–172. https://doi.org/10.1016/j.trac.2018.10.006

17. Hermsen, E., Mintenig, S. M., Besseling, E., & Koelmans, A. A. (2018). Quality criteria for the analysis of microplastic in biota samples: A critical review. *Environmental Science & Technology*, *52*(18), 10230–10240. https://doi.org/10.1021/acs.est.8b01611

18. Horton, A.A., Dixon, S.J., 2018. Microplastics: an introduction to environmental transport processes. Wiley Interdiscip. Rev. Water 5, e1268. https://doi.org/10.1002/wat2. 1268

19. *Lake Tahoe Fun Facts*. Tahoe Fund. (2023, February 15). https://www.tahoefund.org/about-tahoe/tahoe-fun-facts/#:~:text=About%2015%20million%20people%20visit%20Lake%20Tahoe%20each%20year

20. Li, J., Liu, H., & Paul Chen, J. (2018b). Microplastics in freshwater systems: A review on occurrence, environmental effects, and methods for microplastics detection. *Water Research*, *137*, 362–374. https://doi.org/10.1016/j.watres.2017.12.056

21. Li, Y. et al. Airborne fiber particles: types, size and concentration observed in Beijing. Sci. Total Environ. 705, 135967 (2020)

22. Liu, S., Shang, E., Liu, J., Wang, Y., Bolan, N., Kirkham, M. B., & Li, Y. (2021). What have we known so far for fluorescence staining and quantification of microplastics: A tutorial review. *Frontiers of Environmental Science & Engineering*, *16*(1). https://doi.org/10.1007/s11783-021-1442-2

23. Mani, T., Hauk, A., Walter, U., & Burkhardt-Holm, P. (2015). Microplastics profile along the Rhine River. *Scientific Reports*, *5*(1). https://doi.org/10.1038/srep17988

24. O'Brien, S., Rauert, C., Ribeiro, F., Okoffo, E. D., Burrows, S. D., O'Brien, J. W., Wang, X., Wright, S. L., & Thomas, K. V. (2023a). There's something in the air: A review of sources, prevalence and behaviour of microplastics in the atmosphere. *Science of The Total Environment*, *874*, 162193. https://doi.org/10.1016/j.scitotenv.2023.162193

25. Prata, J. C., da Costa, J. P., Duarte, A. C., & Rocha-Santos, T. (2019). Methods for sampling and detection of microplastics in water and sediment: A critical review. *TrAC Trends in Analytical Chemistry*, *110*, 150–159. https://doi.org/10.1016/j.trac.2018.10.029

26. Rezaei, M., Riksen, M. J. P. M., Sirjani, E., Sameni, A. & Geissen, V. Wind erosion as a driver for transport of light density microplastics. Sci. Total Environ. 669, 273–281 (2019)

27. Rolph, G., Stein, A., and Stunder, B., (2017). Real-time Environmental Applications and Display sYstem: READY. Environmental Modelling & Software, 95, 210-228, https://doi.org/10.1016/j.envsoft.2017.06.025

28. Sajjad, M., Huang, Q., Khan, S., Khan, M. A., Liu, Y., Wang, J., Lian, F., Wang, Q., & Guo, G. (2022). Microplastics in the Soil Environment: A critical review. *Environmental Technology & Innovation*, *27*, 102408. https://doi.org/10.1016/j.eti.2022.102408

29. Schwartz, D. L., Mullins, H. T., & Belknap, D. F. (1986). Holocene geologic history of a transform margin estuary: Elkhorn Slough, Central California. *Estuarine, Coastal and Shelf Science*, *22*(3), 285–302. https://doi.org/10.1016/0272-7714(86)90044-2

30. Sun, J., Dai, X., Wang, Q., van Loosdrecht, M. C. M., & Ni, B.-J. (2019). Microplastics in wastewater treatment plants: Detection, occurrence and removal. *Water Research*, *152*, 21–37. https://doi.org/10.1016/j.watres.2018.12.050

31. Surendran, U., Jayakumar, M., Raja, P., Gopinath, G., Chellam, P.V., 2023. Microplastics in terrestrial ecosystem: Sources and migration in soil environment. Chemosphere, 137946.

32. Stein, A.F., Draxler, R.R, Rolph, G.D., Stunder, B.J.B., Cohen, M.D., and Ngan, F., (2015). NOAA's HYSPLIT atmospheric transport and dispersion modeling system, Bull. Amer. Meteor. Soc., 96, 2059-2077, http://dx.doi.org/10.1175/BAMS-D-14-00110.1

33. The State of Queensland. (n.d.). Air quality monitoring - Samplers. Retrieved June 9, 2024, from https://www.qld.gov.au/environment/management/monitoring/air/air-monitoring/measuring/samplers

34. Ward, E., Gordon, M., Hanson, R., & Jantunen, L. M. (2024). Modelling the effect of shape on atmospheric microplastic transport. *Atmospheric Environment*, *326*, 120458. https://doi.org/10.1016/j.atmosenv.2024.120458

35. Zhu, L., Kang, Y., Ma, M., Wu, Z., Zhang, L., Hu, R., Xu, Q., Zhu, J., Gu, X., & An, L. (2024). Tissue accumulation of microplastics and potential health risks in human. *Science of The Total Environment*, *915*, 170004. https://doi.org/10.1016/j.scitotenv.2024.170004